

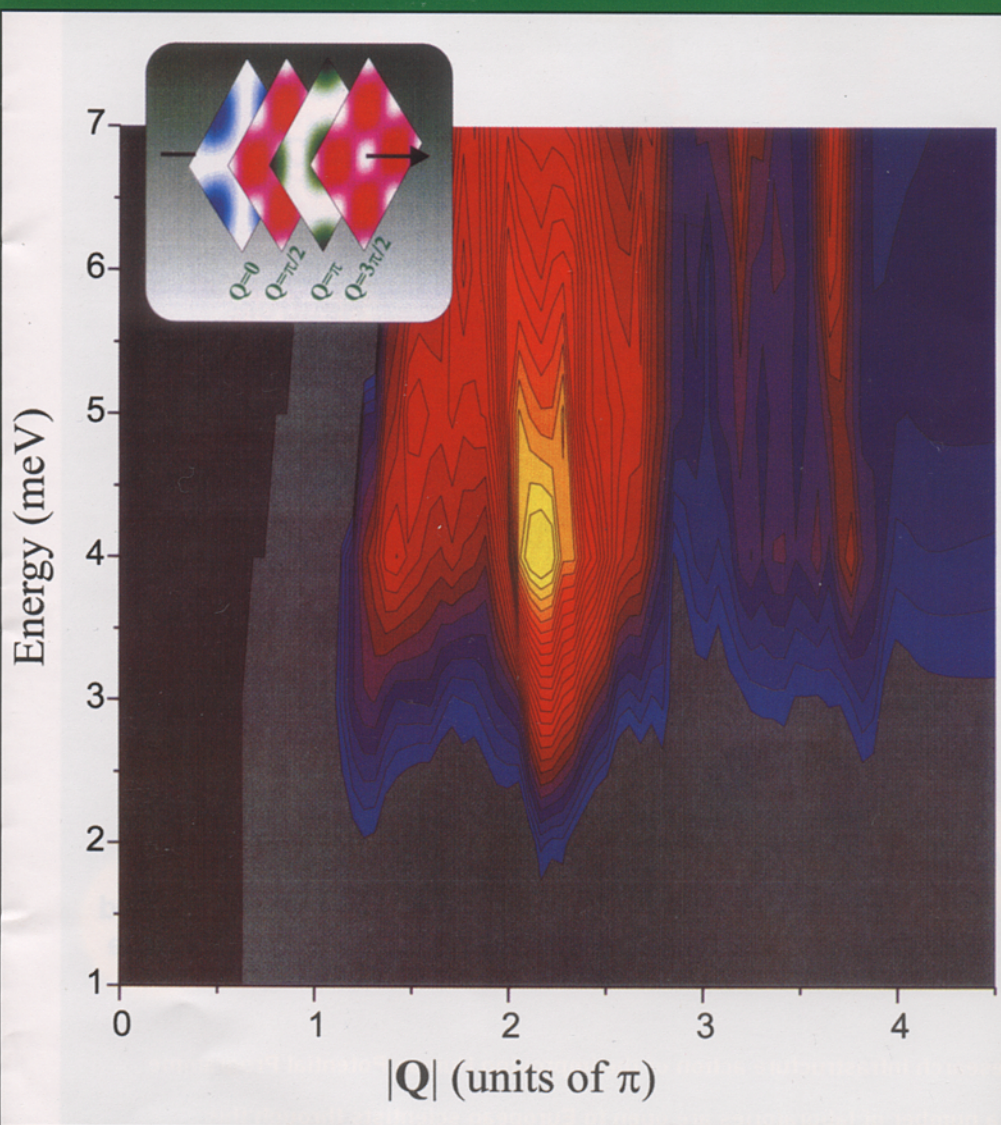
Neutron News

Volume 11, Issue 3

FEATURING
PAUL SCHERRER
INSTITUT

IN THIS ISSUE

- THE CONTINUOUS SPALLATION NEUTRON SOURCE SINQ
- NEUTRON DIFFRACTION AT SINQ
- NEUTRON INELASTIC SCATTERING AT SINQ
- FACILITIES FOR NON-DIFFRACTIVE APPLICATIONS AT SINQ
- NEW FACILITY FOR PARTICLE PHYSICS WITH POLARIZED COLD NEUTRONS



G+B MAGAZINES

Neutron Inelastic Scattering at SINQ

N. CAVADINI¹, A. ZHELUDEV²
and D. RUBIO-TEMPRANO¹

¹ Laboratory for Neutron Scattering
ETH Zurich & PSI, CH-5232 Villigen PSI,
Switzerland

² Physics Department, Brookhaven National
Laboratory, Upton, NY 11973-5000, USA

Spin gap and quantum excitations in the S=1/2 compound TlCuCl_3

Quantum spin systems featuring a singlet ground state and a magnetic excitation gap have been attracting much interest recently, both theoretically and experi-

mentally. Despite the conclusive insights which neutron scattering can provide in such compounds, only a limited number of complete inelastic investigations has been presented so far, mostly due to the absence of large enough single crystals. The clear results obtained from high quality single crystals of the dimer compound KCuCl_3 [1] motivated our interest for the isostructural compound TlCuCl_3 , on which preliminary outcomes collected at SINQ are reported below.

The insulator KCuCl_3 has been recently characterized as a S=1/2 dimer system, with a nonmagnetic singlet ground state separated from well-defined triplet excitations by a spin gap $\Delta \sim 2.7$ meV. The observed energy and intensity of the excitations can be described assuming strong antiferromagnetic dimerization of neighboring spins as the dominant model feature. Weak exchange couplings between the dimers completely account for the dispersion relation of the triplets above the gap Δ . In the presence of a field, these excitations undergo a linear threefold Zeeman splitting and Δ is accordingly decreased. From high field magnetization measurements, KCuCl_3 is known to undergo a quantum phase transition at $B_c \sim 20$ T, which corresponds to the closing of the gap. In the case of the isostructural compound TlCuCl_3 , this closing already occurs at $B_c \sim 6$ T [2], an issue which promotes the system as a potential candidate for the successful neutron study of magnetic interactions near to a quantum critical point.

With the aim of determining the exchange couplings in TlCuCl_3 , zero field measurements have been performed at the cold three-axis spectrometer DrüchLa, which is installed at SINQ (Figures 1 and 2). The intrinsically smaller gap observed at $\Delta \sim 0.9$ meV, accompanied by the enlarged bandwidth of the excitations dispersion indicates that in TlCuCl_3 appreciable spin-spin correlations extend well beyond the dimer cluster.

Accordingly, the unbalance between intra-dimer and inter-dimer couplings is less pronounced. From the dispersion curves collected in the $(h\ 0\ l)$ scattering plane, we were able to determine the model parameters. The effective dimer coupling scheme valid in KCuCl_3 explains the observed singlet-triplet modes in TlCuCl_3 as well, however with different ratios for the exchange coupling constants (Figure 2). A complete account of

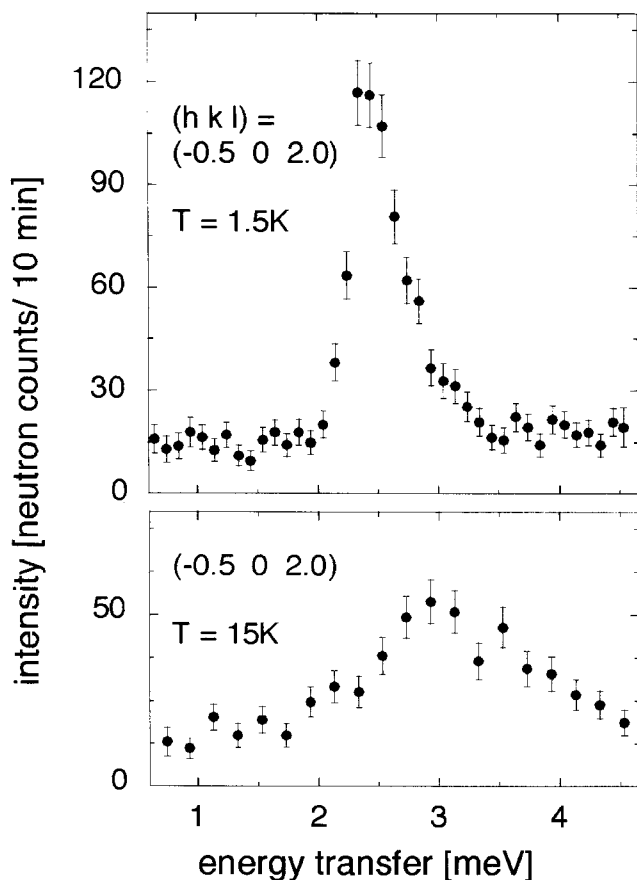


Figure 1. Measured excitations from TlCuCl_3 obtained on DrüchLa at $T=1.5\text{K}$ (above) and $T=15\text{K}$ (below). The renormalization at higher T is indicative of their magnetic nature.

the above investigations, extended to include effects of higher order in the spin-spin interactions, will be reported elsewhere [3]. The resulting dynamical characterization of the magnetic properties in TlCuCl_3 will hopefully be the basis of interesting field investigations.

Magnetic excitations in coupled spin chains near the quantum critical point

It is by now well established that for integer spins, the 1-dimensional (1-D) Heisenberg antiferromagnet (HAF) has a quantum-disordered spin liquid ground state and a so-called Haldane gap in the magnetic excitation spectrum. In recent years the focus has shifted towards studies of more complex *quasi*-1-D systems. Of particular current interest is the quantum phase transition between spin-liquid and ordered states, which occurs when 3-D interactions and/or magnetic anisotropy are increased beyond certain threshold values. The most direct way to observe this phenomenon experimentally is by looking at a series of isostructural compounds with slightly different inter-chain coupling constants or anisotropy terms. Unfortunately, most known quasi-1-D $S = 1$ HAF systems are otherwise deep inside the spin-liquid area of the phase diagram, or obviously in the 3-D ordered phases. Only about a year ago the first quasi-1-D integer-spin, AF, that is still in the spin-liquid state, but on the verge of 3-D ordering instability, was characterized [4]. This material, $\text{PbNi}_2\text{V}_2\text{O}_8$, is so close to the phase boundary that LRO, absent in the pure compound, can be induced by spin-vacancy substitution. Moreover, an isostructural undoped system, namely $\text{SrNi}_2\text{V}_2\text{O}_8$, does order magnetically at low temperatures.

What subtle differences between the two vanadates lead to such vastly distinct ground state properties? An answer to this question was obtained in the studies of quantum magnetic excitations in these materials, performed at the TASP and DrüchAL spectrometers at SINQ. Obtaining information on both in-chain and inter-chain interactions in these quasi-1-D systems turned out to be a formidable challenge, as only powder samples are currently available. Help came from an unexpected direction, namely from the peculiar *spiral* shape of the $S = 1$ Ni^{2+} AF spin chains in $\text{PbNi}_2\text{V}_2\text{O}_8$ and $\text{SrNi}_2\text{V}_2\text{O}_8$ (Figure 3). Rather than being an obstacle, the complicated 3-D structure factor of such spiral chains makes certain features of the powder-averaged inelastic cross section extremely sensitive to even weak inter-chain interactions. Measurements of inelastic spectra for $\text{PbNi}_2\text{V}_2\text{O}_8$ (Figure 3) and $\text{SrNi}_2\text{V}_2\text{O}_8$ [5], and a subse-

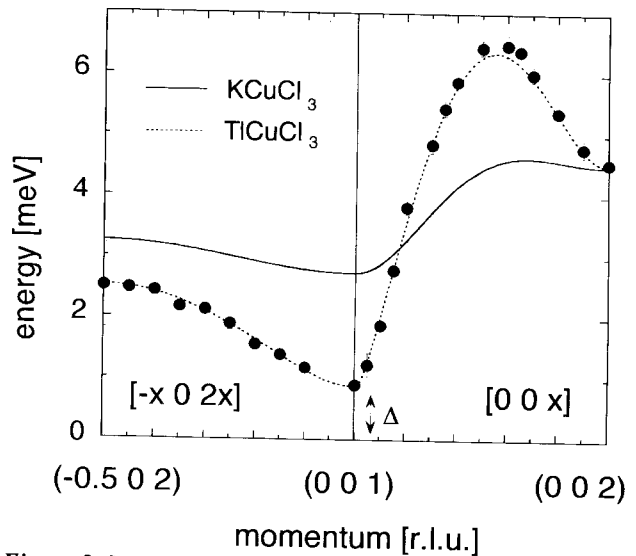


Figure 2. Low-energy cuts from the observed magnetic excitations in TlCuCl_3 (full points). The dispersion relations determined for TlCuCl_3 (dotted line) and KCuCl_3 (continuous line) are compared along selected directions (in reciprocal lattice units).

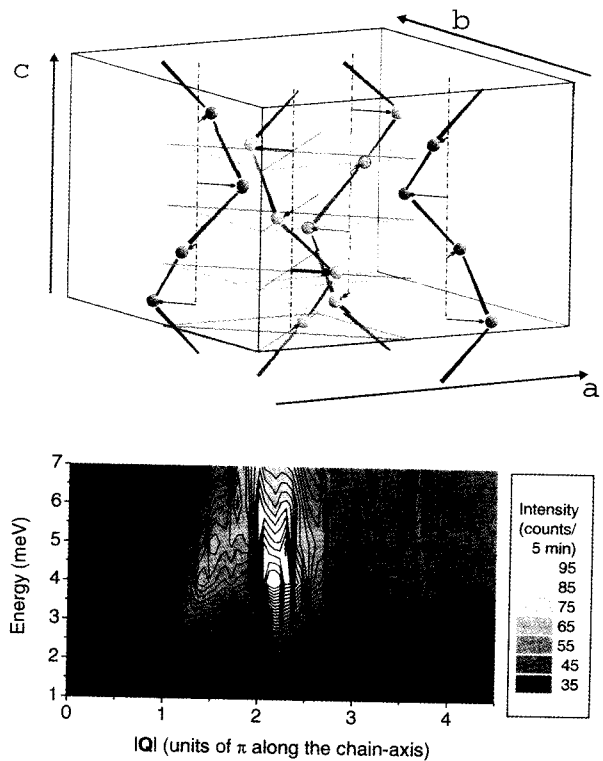


Figure 3. Top: $S=1$ Ni^{2+} magnetic ions in $\text{SrNi}_2\text{V}_2\text{O}_8$ and $\text{PbNi}_2\text{V}_2\text{O}_8$ are arranged in peculiar spiral-shaped AF chains that run along the c axis of the tetragonal structure. Bottom: The inelastic neutron scattering cross section measured in Pb not only gives an estimate of the intrinsic 1-D Haldane gap energy, but carries information on weak inter-chain interactions.

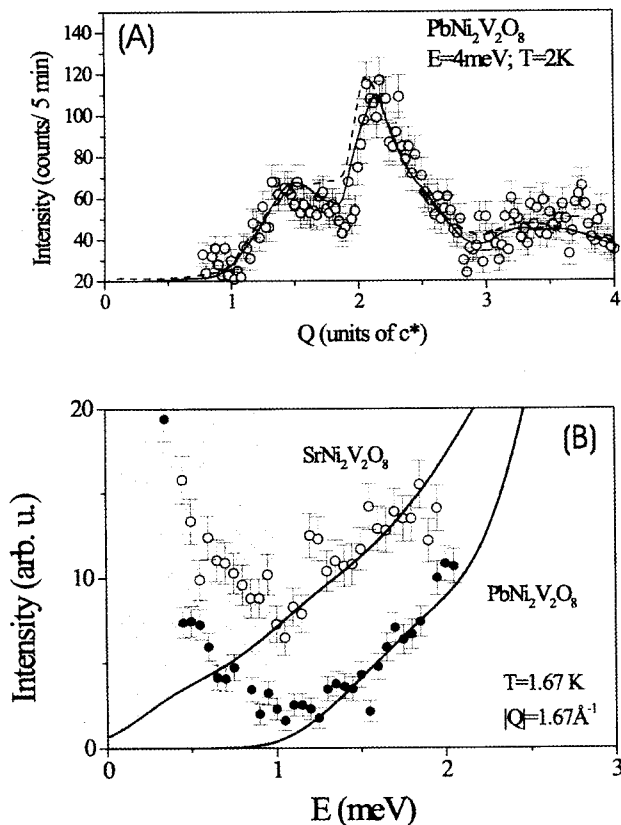


Figure 4. (A) A simple chain-RPA model for weakly coupled chains (solid line) reproduces the characteristic double-peak structure of measured const- Q scans (symbols), while a model based on non-interacting spin chains gives only one distinct peak (dashed line). (B) High-resolution low-energy constant- E scans reveal the presence of a gap in $\text{PbNi}_2\text{V}_2\text{O}_8$ and a gapless spectrum in $\text{SrNi}_2\text{V}_2\text{O}_8$. The solid lines are predictions of the chain-RPA model for both materials. The shaded area is affected by incoherent and thermal-diffuse scattering.

quent analysis based on a chain-RPA model, allowed us to determine the microscopic parameters in the two systems (Figure 4A).

It turns out that the intrinsic (non-interacting) gap energies $D = 3.9$ meV are almost identical in the two compounds. Moreover, contrary to expectations, interchain coupling is actually *weaker* in $\text{SrNi}_2\text{V}_2\text{O}_8$, $|J_{\perp}| = 0.13(2)$ meV, as opposed to $|J_{\perp}| = 0.18(2)$ meV for the quantum-disordered lead-based system. The key feature of $\text{SrNi}_2\text{V}_2\text{O}_8$ that drives it towards long-range magnetic order was found to be the slightly larger easy-axis magnetic anisotropy (~ 0.4 meV, as compared to ~ 0.2 meV in $\text{PbNi}_2\text{V}_2\text{O}_8$). The effect of this increased anisotropy is to split the triplet of the

Haldane-gap excitations and to drive the energy of the lower gap excitation to zero at the 3-D AF zone-center. While $\text{PbNi}_2\text{V}_2\text{O}_8$ retains a gap of ~ 1.2 meV at $T \rightarrow 0$, the excitation spectrum of $\text{SrNi}_2\text{V}_2\text{O}_8$ is gapless (Figure 4B).

The basic physics of these exciting new quantum magnets is now well understood; future studies of aligned powders and high-pressure experiments will enrich our knowledge of the unique “quantum-classical” transition in weakly-coupled quantum spin chains. Part of this work was done at Brookhaven National Laboratory and carried out under Contract No. DE-AC02-76CH00016, Division of Material Science, U.S. Department of Energy.

Pseudogap in a back-exchanged $\text{HoBa}_2\text{Cu}_4\text{O}_8$ compound: confirmation of a large isotope effect

The underdoped high-temperature superconductors are characterized by the presence of correlations in the normal state giving rise to a pseudogap at $T^* > T_C$ and a reduced density of states above T_C . The existence of a pseudogap is considered to be amongst the most important features of cuprates, since it may contain the key for the understanding of these materials. Experimentally, the most convincing pseudogap data have been obtained by ARPES measurements in Bi2212 compounds, NMR and NQR results in Y124 compounds, as well as neutron spectroscopic measurements in Ho124 and Er247 compounds. Despite of all this experimental work, the physi-

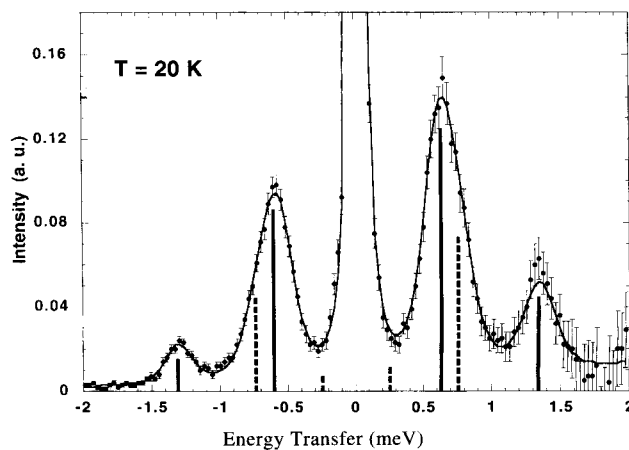


Figure 5. Energy spectrum obtained on FOCUS for $\text{HoBa}_2\text{Cu}_4^{18}\text{O}_8$ at 20 K. The solid line is the result of a least-squares fit to the data as explained in detail in ref. [6]. The solid and dashed vertical bars indicate the energy and intensity of the ground and excited state crystal-field transitions, respectively.

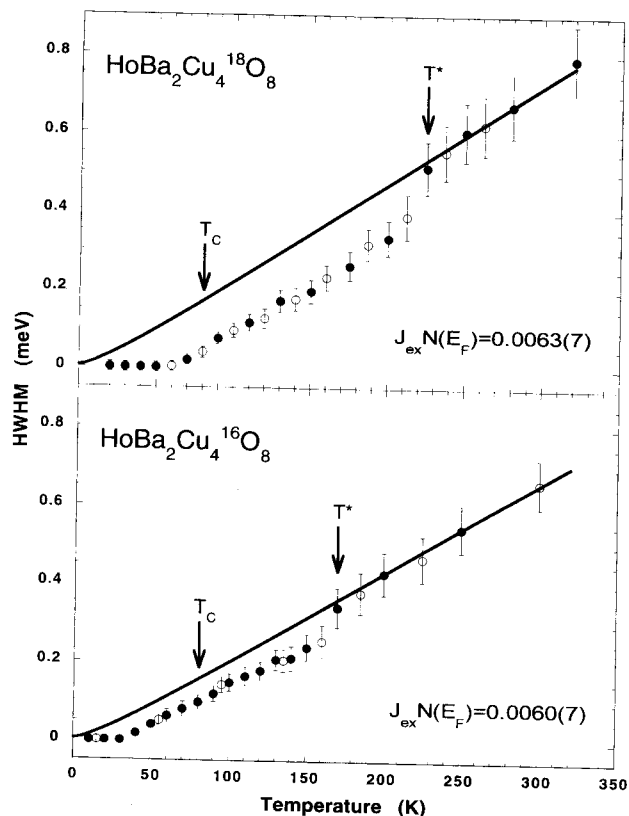


Figure 6. Temperature dependence of the intrinsic linewidth of crystal-field transitions measured for $\text{HoBa}_2\text{Cu}_4^{18}\text{O}_8$ and $\text{HoBa}_2\text{Cu}_4^{16}\text{O}_8$.

cal origin of the pseudogap still remains unclear, and experiments on the isotope effect of the pseudogap may provide crucial information to discriminate between the different proposed models for the pseudogap.

Recently, we have performed such investigations in the slightly underdoped $\text{HoBa}_2\text{Cu}_4\text{O}_8$ compound [6]. By studying the temperature dependence of the intrinsic linewidth of crystal-field transitions, we found a large isotope effect on the pseudogap of $\Delta T^* \sim 50$ K. This result may be an indication that electron-phonon interactions or local lattice fluctuations have to be somehow

involved in the pairing mechanism.

The inelastic neutron scattering experiments have been performed on the hybrid time-of-flight spectrometer FOCUS at SINQ. The instrument was operated in the TF002 mode (time focusing at the elastic line using the 002 reflection of the monochromator). The incident neutron energy was set to 3.27 meV, giving an instrumental resolution (FWHM) of 90 μeV at the elastic position. A closed-cycle refrigerator was used to achieve temperatures in the range $25 \geq T \geq 300$ K. The raw data have been corrected according to standard procedures.

Figure 5 shows the energy spectra of neutrons scattered from $\text{HoBa}_2\text{Cu}_4^{18}\text{O}_8$ at 20 K. All crystal-field states are singlets and result from the decomposition of the seventeenfold degenerate ground state multiplet $^5\text{I}_8$ due to the orthorhombic symmetry. Figure 6 shows IN5 and FOCUS results for the intrinsic linewidth (HWHM) corresponding to the ground state transition $\Gamma_3^{(1)} \rightarrow \Gamma_4^{(1)}$. For the ^{16}O compound, the FOCUS data corresponds to the isotope back-exchanged sample. The nice consistency of this set of data when compared with the data from the original ^{16}O compound confirms the stability of the “1248” family against oxygen isotope substitution, as well as the reliability of the present data.

The huge isotope effect $\Delta T^* \sim 50$ K strongly supports that electron-phonon induced effects play an important role in high-temperature superconductivity. Indeed, a recent theoretical model [7] is able to explain quantitatively ΔT^* and the extremely fast underlying time scale.

References

1. N. Cavadini, W. Henggeler, A. Furrer, K. Krämer, H.U. Güdel and H. Mutka, *Eur. Phys. J. B* **7**, 519 (1999).
2. H. Tanaka, K. Takatsu, W. Shiramura, T. Ono, T. Kambe, K. Kamishima, H. Mitamura and T. Goto, *Physica B* **237-238**, 120 (1997).
3. N. Cavadini et al., in preparation for *Phys. Rev. B*.
4. Y. Uchiyama, Y. Sasago, I. Tsukada, K. Uchinokura, A. Zheludev, T. Hayashi, N. Miura and P. Böni, *Phys. Rev. Lett.* **83**, 632 (1999).
5. A. Zheludev et al., *Phys. Rev. B* (submitted).
6. D. Rubio-Temprano et al., *Phys. Rev. Lett.* **84** (2000) 1990.
7. A. Bussmann-Holder et al., *Phys. Rev. Lett.* (submitted).